12-1-2021

ESTIMATING THE POWER PRODUCED BY A ROOF MOUNTED WIND TURBINE IN AN URBAN SETTING

Kyle Reed Ozier
Southern Illinois University Carbondale, kozier94@outlook.com

ESTIMATING THE POWER PRODUCED BY A ROOF MOUNTED WIND TURBINE IN AN URBAN SETTING

By

Kyle R. Ozier

B.S., Southern Illinois University Carbondale, 2017

A Thesis
Submitted in Partial Fulfillment of the Requirements for the
Master of Science Degree

Department of Mechanical Engineering and Energy Processes

in the Graduate School

Southern Illinois University Carbondale

December 2021

THESIS APPROVAL

ESTIMATING THE POWER PRODUCED BY A ROOF MOUNTED WIND TURBINE IN AN URBAN SETTING

By

Kyle R. Ozier

A Thesis

Submitted in Partial Fulfillment of the Requirements

for the Degree of

Master of Science

in the field of Mechanical Engineering

Approved by:

Chair, Dr. James Mathias

Dr. Kanchan Mondal

Dr. Hossein Eslamiat

Graduate School

Southern Illinois University Carbondale

August 1, 2021

AN ABSTRACT OF THE THESIS OF

Kyle R. Ozier, for the Master of Science degree in Mechanical Engineering, presented on August 1, 2021 at Southern Illinois University Carbondale

TITLE: ESTIMATING THE POWER PRODUCED BY A ROOF MOUNTED WIND TURBINE IN AN URBAN SETTING

MAJOR PROFESSOR: Dr. James Mathias

Growing concern over the effects of carbon emissions and resulting climate change have highlighted the need to move away from fossil fuels and towards renewable sources of energy. Wind energy is a popular and proven renewables technology that it is mostly implemented in rural environments. For urban settings, building mounted wind turbines could be a solution as a local source of renewable energy generation. In this study, the open-source Computational Fluid Dynamics software OpenFOAM is used to determine the wind speed on a high-rise rooftop. The simulation results are then used in tandem with real wind data from the 2020 calendar year to determine the performance of a turbine on the roof of the building. The reference turbine is the QuietRevolution QR6 vertical axis wind turbine, a real commercial turbine with an energy rating of 7 kW. The total annual energy yield was calculated to be 42,557 kWh. In addition to the energy calculations, brief analyses were performed on the spacing requirements of the turbine and on the vibration behavior of the building frame and future research is suggested.

ACKNOWLEDGEMENTS

To my friends and colleagues Jared Wagoner, Kyle Heller, and Austin Peterson, thank you for taking this journey with me.

To my friend and colleague Kshitij Amar, thank you for all the time spent in your office, and for the ideas and conversations that we shared.

To my good friend Benjamin Stremming, thank you for being a sounding board for my ideas and for your architectural expertise.

To my advisor, Dr. Mathias, thank you for encouraging me to finish the goals that I set for myself four years ago, and for believing in me at a time when I did not believe in myself.

To my loving partner, Rebecca Moseley, thank you for supporting me, pushing me, and staying by my side throughout this process.

And to my family, thank you for everything you do for me. I would never have completed this without your support.

TABLE OF CONTENTS

LIST OF FIGURES

LIST OF TABLES

NOMENCLATURE

HAWT = Horizontal Axis Wind Turbine

VAWT = Vertical Axis Wind Turbine

TSR = Tip Speed Ratio

C_p = Power Coefficient

P = Power

CFD = Computational Fluid Dynamics

BIWT = Building Integrated Wind Turbine

SWT = Small-scale Wind Turbine

ABL = Atmospheric Boundary Layer

CWE = Computational Wind Engineering

RANS = Reynolds-Averaged Navier-Stokes

TKE = Turbulent Kinetic Energy

LES = Large-Eddy Simulation

U = Velocity

Z = Elevation

H = Building height

α = Power law coefficient

Z_0 = Aerodynamic roughness height

u^* = Friction velocity

d = Displacement height

κ = Von Karman constant

CAD = Computer Aided Design

U_T = Velocity at Turbine height

λ_f = Front area density

λ_p = Plane area density

σ_H = Standard deviation of building height

ASHRAE = American Society of Heating, Refrigerating and Air Conditioning Engineers

δ = Boundary layer thickness

NOAA = National Oceanic and Atmospheric Administration

NACA = National Advisory Committee for Aeronautics

AMI = Arbitrary Mesh Interface

ANSI = American National Standards Institute

CHAPTER 1

INTRODUCTION

INTRODUCTION

A global effort to reduce carbon emissions has led to a rise in the development and installation of renewable energy sources. Population growth and increasing energy demand have created a sense of urgency for society to shift away from fossil fuels to reduce the impact of global climate change. Cities and other dense urban environments are home to a significant portion of the global population and account for roughly 70% of energy consumption [1]. Thus, these areas provide a logical starting point when determining locations to integrate renewable energy technology.

Wind energy is the result of creating power from the natural movement of air. The production of mechanical power from wind has existed within human society for several hundred years, such as the sails on a ship or windmills for grinding grain. The first devices capable of converting the kinetic energy from wind into electricity were developed in the late 19th century and could produce about 12 kilowatts of power [2]. The development and implementation of wind energy technology continued to improve throughout the 20th century. Existing utility scale wind turbines generally produce 2-3 megawatts [2], and the General Electric company recently launched a massive offshore turbine, the Haliade-X, rated for 12 megawatts of power. According to the International Renewable Energy Agency 2019 report, offshore and onshore wind energy now have a combined capacity of over 622 gigawatts, compared to only 177 gigawatts in 2010 [3]. The wind energy market offers effective and well-established technologies, as well as a strong economic foothold, making it an attractive option as society attempts to increase renewables capacity and reduce the use of fossil fuels.

Most existing wind power installments can be found offshore or in rural environments with steady, unperturbed winds and relatively low surface roughness (i.e. limited obstructions, trees, buildings etc.); however, wind energy has yet to make a significant impact in urban areas. While the concept of urban wind energy has been explored in some capacity, it has yet to become a realistic option for several reasons. Firstly, traditional horizontal axis wind turbines (HAWTs) are considered to be a poor fit for urban environments due to their size, appearance, and noise levels [4]. Additionally, the direction and speed of airflow in cities changes at a high frequency compared to rural environments. The variability in wind direction is particularly problematic for HAWTs, which use tracking systems to orientate the blades to the direction of oncoming wind. This process is known as "yawing". Vertical axis wind turbines (VAWTs) have a rotation axis that is perpendicular to airflow, which allows for the blades to capture wind energy coming from any angle. Furthermore, VAWTs are less noisy than HAWTs and have a more compact design that would be easier to integrate into a city-like infrastructure. Integrating renewable micro-generation projects into the urban complex will move power supply closer to consumers, reduce strain on the local grid and promote the idea of sustainable building design for a green future [5,6].

OVERVIEW

Wind energy is a term used to describe the process of harvesting kinetic energy from the wind to generate mechanical work, which is then converted to electricity. Wind turbines are the mechanical structures that make this process possible. The general components of a wind turbine include the rotor (blades), generator (controls, gearbox, electric generator), and structural components (tower, supports). The blades capture oncoming wind energy and convert it to rotational energy. Resulting rotation of the rotor shaft is converted in the gearbox from low-

speed rotational energy to the high-speed rotations used in the electrical generator to produce electricity.

Wind energy is a renewable source of power, so there are no greenhouse gas emissions formed in the process of converting wind to electricity. A global effort to move society away from fossil fuels has created a surge in the research and development of renewable energy technologies. Wind has been an established source of power since the 1970s and has seen rapid growth in recent years [2]. However, there are several challenges to overcome when considering wind as a potential renewable power source in urban environments. One of the main problems with urban wind is designing and developing a suitable turbine for the given sites. The vast majority of existing wind power is generated by horizontal axis wind turbines, often in large wind farms that function on flat, open terrain that is far from urban areas [5]. HAWTs are a poor fit in cities for many reasons, primarily the inability to capture winds from a variety of angles. A standard wind tracking, or 'yawing' system, would not function well due to the high frequency with which urban winds shift direction. Furthermore, HAWTs are less suited to withstand strong gusts of wind due to the length of the blades, leading to increased stress and fatigue on the rotor. Strong gusts can cause shutdowns in the turbine as well, to avoid excessive stress which may damage parts of the turbine. This wind speed threshold is referred to as the cut-off speed, and is generally in the range of 20-30 m/s (approximately 45 – 67 mph). Conversely, the cut-in wind speed is the wind velocity at which the turbine starts performing. Most wind turbines have a cut-in speed in the range of 5 m/s (11 mph) [7]. Other important parameters when evaluating the performance of wind turbines include the tip speed ratio (TSR) and power coefficient (C_p), and swept area of the blades [8]. TSR describes the ratio between tangential speed of the blade tip and the incident wind velocity, and C_p is an efficiency term describing the energy produced by

the turbine relative to the available wind power. Traditional HAWTs operate at higher C_p values when compared with VAWTs, as well as much higher TSR [9]. Although greater power coefficients are preferred, high tip speed ratios are associated with increased noise levels and mechanical fatigue, which is undesirable in densely populated urban areas. VAWTs can also achieve lower cut-in speeds and operate under exposure to strong gusts without sustaining significant damage, which is important in the unpredictable winds that are present in urban settings. For these reasons, vertical axis wind turbines have been considered a prime candidate for use in urban micro-generation [5,10].

Because VAWTs have a rotation axis that is perpendicular to oncoming winds, it allows for the capture of energy from any angle, meaning that no controls system is necessary to orient the device to the oncoming wind. VAWTs have been able to achieve lower cut-in speeds and can be designed to withstand stronger wind gusts [5]. They also have lower tip speed ratios compared to HAWTs, which helps minimize the mechanical stresses on the blades and reduces noise. Additionally, the generator components are at the base of the VAWT tower, allowing for easy access when maintenance is required. Some of the primary drawbacks and challenges of typical VAWT designs include poor power efficiency, fatigue on the blades due to long-term exposure to high turbulence levels, and economic feasibility [10].

There are two primary classifications of VAWT design: the Savonius wind turbine and the Darrieus wind turbine. Savonius wind turbines typically consist of two or three blades in the shape of a half cylinder, which catch the incident wind streams. The resultant drag forces on the blades then spin the rotor. The Savonius turbines operate at low cut-in speeds and require no self-starting mechanism, and as such are the best turbine option for sites with low wind speeds. The major drawback of Savonius turbine designs is relatively poor efficiency and power output

[5,11]. Another VAWT design, the Darrieus turbine, utilizes lift forces rather than drag forces, making it capable of higher efficiencies than the Savonius turbine. The lift-based design demonstrates increased tip-speed ratios and superior aerodynamic performance when compared to drag-force turbines [12]. Several iterations of the Darrieus turbine have been developed. One of the most popular designs is the H-Darrieus turbine, which consists of two or three blades which are parallel to the axis of rotation, connected to the main shaft via armatures. Another lift-based turbine design, the Gorlov turbine, is essentially a modified version of the H-Darrieus turbine. Gorlov turbines incorporate helical shaped blades that twist around the axis of rotation. Benefits of the helical blade design include diminished stress and vibration, and lower starting torque. The main disadvantage is the cost associated with manufacturing airfoils with such a complex geometry [12].

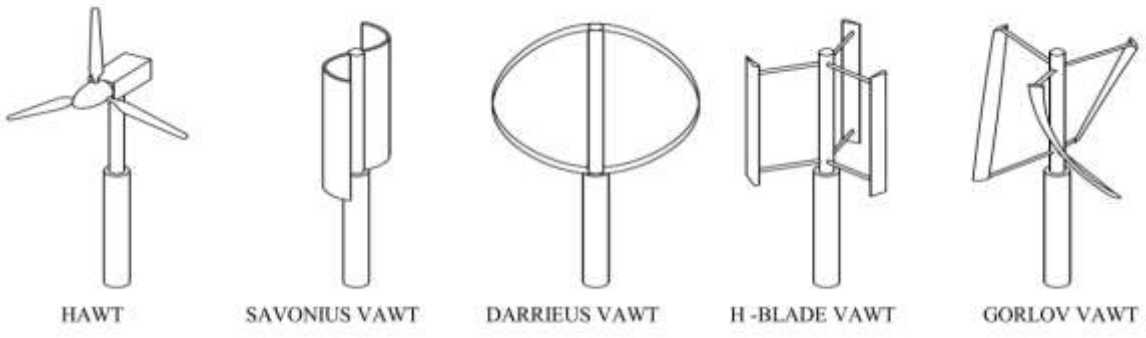

Figure 1: Wind Turbine Designs [13]

Figure 1 displays various turbine designs. No matter what wind turbine is being installed, a thorough assessment of the available wind resources must be performed to properly predict the power output of a wind turbine at a potential site. The maximum available power in a cross-section of wind is simply the kinetic energy of the airstream, which can be described as a function of air density, area (swept by the turbine), and wind speed, as shown in Equation (1).

$$P_W = \frac{1}{2}\rho A v^3 \quad (1)$$

Because velocity is a cubic term in this equation, small variances in wind speed translate to large differences in available energy. This highlights the importance of accuracy when evaluating wind speeds at a potential turbine site. The preferred and most reliable practice for wind assessment would be to take on-site measurements; however, such studies require adequate time and funding to complete. Another popular method for predicting wind behavior is wind tunnel testing. Wind tunnel models are cheaper than field testing, and multiple iterations may be performed in a reasonable amount of time. However, they are still subject to size and scale limitations. A more modern approach is to perform a simulation using computational fluid dynamics (CFD) modeling software. CFD was introduced as a numerical approach to study complex fluid mechanics. It is primarily based on the Navier-Stokes equations for fluid flow. Modern computing now enables researchers to perform robust CFD simulations that incorporate a wide range of customizable input parameters, such as turbulence models and built geometry, to accurately predict fluid flow. CFD simulations are far quicker and cheaper than on-site testing, and the ability to simulate geometry at real size is beneficial when analyzing a built urban landscape. The most commonly used software for performing CFD simulations are the commercial packages Ansys Fluent or Ansys CFX, and the open-source software OpenFOAM [14].

JUSTIFICATION OF RESEARCH

Research on renewable energy is significant for several reasons. Most importantly, humans must reduce the use of fossil fuels to limit the amount of carbon dioxide entering the atmosphere. Climate change is quickly becoming a global crisis and an increase in zero emission

energy sources can have a positive impact for all. Urban centers are one of the highest density areas for end-use energy, and they have limited space to build traditional power production sites. Therefore, the implementation of micro-generation stations is an attractive solution when looking to implement renewable energy sources in heavily built and populated areas. Rooftop wind turbines could be installed on existing structures, and no major updates to the buildings and surrounding environment would be required. Thus, research on the feasibility and performance of turbines at these sites is necessary. This paper may serve as a benchmark study for performance evaluation of a modern VAWT design in an urban environment and provide a blueprint for analyzing rooftop energy potential in coastal settings.

OBJECTIVES

The goal of this study is to evaluate the performance of a commercially available VAWT mounted on the roof of a downtown high-rise building, near a large body of water. The wind behavior and values of interest will be analyzed using the open-source CFD software OpenFOAM. To carry out this study, the following objectives and tasks have been defined.

1. Create the building model and wind domain.
2. Setup the CFD simulation in OpenFOAM.
3. Run simulations at each wind speed and record data for velocity above the rooftop.
4. Develop velocity profiles for atmospheric boundary layer
5. Calculate energy yield of turbine.
6. Discuss results and suggest future work.

In addition to the goals listed above, a brief analysis will be performed on the vibration behavior of the building frame and on the spacing requirements for multiple turbines.

CHAPTER 2

LITERATURE REVIEW

URBAN WIND ENERGY

Urban wind energy can be described as the generation of power using relevant wind engineering technologies integrated into the built environment. This can include devices installed at the ground level or attached to existing structures. Because densely populated urban areas constitute a significant percentage of global energy use, there has been increased interest in the development and installation of urban micro-generation projects. More specifically, building integrated wind turbines (BIWT) have emerged as a potentially viable option for renewable energy production. Successfully integrating renewable energy generation onto urban structures, such as high-rise buildings, will decrease electrical costs for the building and lessen the load on the central power grid. Additionally, it promotes green energy solutions and the idea of sustainable building design. Such concepts have become increasingly relevant as society works to reduce carbon dioxide emissions [5,6].

The behavior of air flow in a complex urban setting is much less predictable because of the increased surface roughness within the Atmospheric Boundary Layer (ABL). Because of this, the mean wind speed in cities is typically less than at rural sites, and the turbulence levels are much higher. Turbulent gusts contain large bursts of available power, and it has been demonstrated in multiple studies that optimized controls systems could greatly enhance the performance of wind turbines in locations with high turbulence intensity [15,16]. Urban landscapes tend to generate augmented flow over and around buildings/structures, and these regions will produce high velocity wind streams that contain a suitable power density for efficient and consistent energy harvesting. Several studies have been conducted to gain

additional insight regarding the potential of BIWTs. A CFD-based study published in 2011 by Ledo et al. examined the changes in velocity and turbulence intensity for wind flowing over different roof shapes; flat, pitched, and pyramidal. The authors determined that the area above flat roofs have faster air streams with a consistently higher power density when compared with other roof shapes, regardless of incident wind angle [17]. Furthermore, a 2011 study on the feasibility of a rooftop mounted VAWT found that significant improvements to turbine performance occurred when the target building was substantially taller than the surrounding buildings [18]. Thus, it can be concluded that high-rise buildings in urban environments present an attractive option when searching for potential turbine mounting sites. A recent paper by Rezaeiha et al. puts forth a general framework for estimating rooftop wind energy potential [19].

Utility scale wind turbines, such as those observed in a typical onshore wind farm, are widely accepted in rural settings where the wind is steady, high speed, low in turbulence, and the relative surface roughness of the surrounding area is small. However, these larger turbines are a poor fit for urban environments due to their size. Small-scale wind turbines (SWT) present an attractive alternative for urban use, as they can be safely installed on or around the existing infrastructure. The Renewables 2019 Global Status Report has shown a steady increase in global SWT capacity, including 161 megawatts of small-scale wind power installed in the previous two years. Moreover, despite being limited in research and development when compared to standard utility scale wind turbines, economic benefits in the form of tax credits will hopefully incentivize building owners to invest in small-scale wind power devices. This should ensure that the market for SWT research, development, and installation continues to see steady growth [20].

SUMMARY OF SMALL-SCALE VERTICAL AXIS TURBINES

As previously discussed, HAWTs have experienced widespread commercial success and are capable of high efficiencies, but they are still considered a poor choice in urban settings. This is primarily due to subpar performance in unsteady velocity profiles, and heightened levels of mechanical stress from repeated exposure to turbulence, among other reasons. Conversely, VAWTs exhibit several characteristics that are beneficial for operating within the built environment, e.g. omnidirectional energy capture, lower noise levels, stable performance in erratic winds, reduced risk of fatigue failure, and a more aesthetically pleasing appearance [5]. Despite these traits, there are still drawbacks to the VAWT that have inhibited their development and market expansion. Downsides include lower rated power coefficients (compared with HAWTs), unwanted vibrations from turbine torque ripple affecting the building or structure, and higher associated costs. Kumar et al. published a comprehensive review of vertical axis wind turbines for purposes of urban wind energy research [5].

VAWTs are typically classified by their working principle, i.e. lift force or drag force on the rotors. The Savonius wind turbine incorporates a drag-based design and was the earliest VAWT concept to be developed. The design was first introduced by Sigurd Johannes Savonius in 1922. Positive attributes of the Savonius turbine include the relatively simple design, manufacturing, and installation processes, as well as having low cut-in wind speeds (typically around 2 m/s or 4.5 mph). Because of this low starting torque, Savonius turbines require no self-starting mechanism and are known for their respectable performance in locations with low average wind speeds. The primary disadvantage of the Savonius design is the extremely low tip speed ratio (TSR), which cannot exceed a value of one for drag-based rotors. Higher TSR is associated with improved power output, so this greatly limits the potential yield and efficiency of

Savonius turbines. A typical Savonius turbine may have a power coefficient rating of 0.15, with a standard range of 0.1 – 0.25. Other notable design aspects that effect the performance are the number of blades and the overlap ratio. A 2017 paper by Zemamou et al. provides a comprehensive review of Savonius designs and performance parameters, as well as suggesting some potential improvements to existing designs [11]. More modern concepts involve Savonius turbines with helical blade profiles, or the pairing of a Savonius rotor within a lift-based turbine to create a hybrid VAWT [5,13]. Regarding commercially available devices, the top performing drag-force turbine designs are rated for about 4.5 kilowatts at wind speeds around 14 m/s (31 mph), and cut-in speeds of 1.5 m/s (3.35 mph). Additionally, some helical shaped Savonius turbines are capable of similar power ratings at lower wind speeds (~7 m/s or 15.5 mph), although they also require a greater start-up wind speed, typically 4-5 m/s (9-11 mph) [13].

The Darrieus turbine design is a lift-based wind power device that has demonstrated greater power conversion efficiency in comparison to Savonius and other drag-force VAWT concepts. The Darrieus wind turbine was first conceived by French engineer Georges J.M. Darrieus in 1931. The original designs included both a curved-blade and straight-blade rotor concept for the turbine. Kumar et al. published an extensive review on the development of small Darrieus wind turbines and the various types [5]. The straight-blade design is often referred to as an H-Darrieus turbine, and is the simplest Darrieus concept in terms of manufacturing and assembly [12]. H-Darrieus turbines are proven to demonstrate greater power coefficients (0.25 – 0.35) than Savonius and other drag-force turbines. Despite this, there are reasons to doubt the suitability of Darrieus turbines for urban application, specifically regarding rooftops [12]. The major concern hindering urban application of Darrieus turbines is the high starting torque of H-rotor designs. Dominy et al. performed a study on the self-starting behavior of two and three-

bladed H-Darrieus turbines. The authors observed that the three-blade design was capable of self-starting from any orientation (wind angle) for a given wind speed, while the two-blade turbine was only able to start from certain positions. Furthermore, the three-bladed turbine was capable of self-starting at lower wind speeds than the two-bladed turbine [21]. Despite these improvements, the cut-in speed of straight-blade Darrieus turbines (~ 4 m/s or 9 mph) is still much higher than that of Savonius turbines, and they often require some form of self-starting mechanism when operating in areas with lower mean wind speeds.

Some innovative VAWT designs have been developed which offer improved performance over the more standard turbines. An alteration to the straight-blade Darrieus design is a helical blade profile that twists about the axis of rotation. The helical design, known as a Gorlov turbine (or simply a helical Darrieus turbine), demonstrates improved self-starting capabilities. Helical Darrieus turbines have achieved cut-in wind speeds similar to that of Savonius turbines, around 1.5 m/s (3.35mph). Additionally, the blade profile demonstrates lower noise levels, reduced vibrations and reduced stress on the blades [12]. Wind tunnel experiments on helical Darrieus turbines have shown suitable efficiencies as well, achieving C_p values as high as 0.4 [22]. A relatively new commercial turbine that incorporates helical blades, the QR6 by QuietRevolution, is rated for 7 kilowatts. Furthermore, it has a cut-in speed of 2 m/s and can survive in wind speeds up to 52.5 m/s (117 mph) [12]. The QR6 is optimized to operate in winds ranging from 10 m/s – 16 m/s (22-36 mph) and has a built-in cut-off when wind speeds exceed 20 m/s (45 mph). Another concept is the combined Savonius-Darrieus wind turbine, which takes advantage of the low starting-torque of the Savonius rotor, while offering the performance advantages of the Darrieus design at higher wind speeds. Hi-VAWT Technologies Corp. offers multiple hybrid turbines which incorporate an S-Savonius rotor within a curved Darrieus rotor.

The DS-700 is rated for 700 watts at wind velocity of 10 (22mph), and has a cut-in speed of 2 m/s (4.5 mph) [5]. The company's newest model, the DS-3000, is rated for 3 kilowatts and offers similar performance parameters.

COMPUTATIONAL FLUID DYNAMICS IN WIND ENGINEERING

Since its conception, Computational Fluid Dynamics has been an important tool applied to wind engineering applications. The use of CFD for wind engineering purposes is sometimes referred to as Computational Wind Engineering (CWE). A comprehensive review written by Bert Blocken details the history of CWE, outlines best practice guidelines for CFD approaches to wind engineering projects, and discusses the future of the field [23]. CFD software packages provide researchers with a viable way to analyze the wind behavior associated with a given project, without the time and resources necessary to perform live experiments. CFD simulations can also be performed with real size geometry, unlike wind tunnel testing, which is another popular method for flow analysis. However, CFD can yield flawed and inconsistent results due to the number of parameters that must be defined by the user. It is imperative that the user know the right techniques for setting up a CFD simulation. Examples of important user choices include selecting an appropriate turbulence model, creating an accurate velocity profile within the atmospheric boundary layer, and defining the boundary conditions and domain size. It is also important to develop a proper mesh to achieve high quality results. Access to adequate computing power can sometimes limit the scope and quality of CFD simulations, especially for certain turbulence models and for very fine meshes. Despite the many advantages of a CFD approach, the models and techniques used are still being refined, and the accuracy of CFD simulations can be highly sensitive to user input. Additional research within the field is needed to validate different simulation methods [23].

TURBULENCE MODELS

An extensive review of CFD research with a focus on urban wind energy exploitation was published in 2018 by Toja-Silva et al. [14]. In section 2 of the paper, the authors review different turbulence models and their performance with respect to CFD simulations. More than 50% of the studies highlighted in the article use Reynolds-Averaged Navier-Stokes (RANS) turbulence models. There are multiple turbulence models derived from the RANS equations, many of which are pre-programmed into CFD software packages. A popular example is the two-equation realizable k-epsilon RANS turbulence model, where epsilon describes the turbulence dissipation rate. The k-epsilon model has several variations; SKE, Realizable, and RNG are the most well documented [24]. Additionally, many researchers over time have developed different values for the model coefficients that appear in the RANS equations. The k-omega (shear stress transport, or SST) RANS turbulence model is also frequently used in CFD wind simulations, and like the k-epsilon model it has multiple variations. Toja-Silva et al. performed a validation and comparison of many RANS turbulence models on an isolated building rooftop [24]. The results showed that all versions of the k-epsilon model tested met the validation criteria for velocity, however not all models adequately evaluated Turbulent Kinetic Energy (TKE). The authors state that TKE is an important factor when trying to predict future damage to the turbine. Large-Eddy Simulation (LES) is another well-established turbulence model that has demonstrated high quality results – however, it is much more computationally intensive than the k-epsilon or k-omega turbulence models, and therefore not used as often. When a turbulence model is selected in the CFD simulation setup, default values for the coefficient terms will be applied to the RANS equations, unless alternate values are defined by the user.

A study published in 2016 compared the results of a CFD simulation with on-site measurements in an urban area in Taipei, Taiwan. Researchers compared values for wind speed, wind direction, and turbulence intensity , and found that the realizable k-epsilon turbulence model provided better results for turbulence intensity than other k-epsilon variations, and the wind speed was less than 10% difference when compared with on-site measurements. Second-order upwind discretization should be used in the CFD solver, combined with two equation k-epsilon turbulence models in order to obtain best results [14].

VELOCITY PROFILE OF ATMOSPHERIC BOUNDARY LAYER

The velocity profile can be difficult to model, especially when considering the complexities of the built urban environment. The velocity profile will develop within the atmospheric boundary layer, with lower speeds occurring near the ground and faster speeds at higher elevations. The finer details of the velocity profile will depend on the relative roughness of the earth's surface at a given location. For open terrain, a classic exponential profile is usually acceptable.

$$U = U_{ref} \times \left(\frac{z}{z_{ref}}\right)^{\propto} \quad (2)$$

From this equation, velocity (U) can be determined at any elevation (z) by knowing a reference velocity (U_{ref}) at a given elevation (z_{ref}) [25]. Alpha (α) is the power law coefficient, which is usually a predetermined value for a given surface type i.e. land, body of water, etc. However, in urban areas there are more obstacles within the roughness sublayer of the atmospheric boundary layer that affect the velocity profile. For built environments, the power law relationship tends to overestimate velocity below the average building height (H_{ref}), and underestimate the wind speeds above it [17]. In these situations, a semi-log profile is used to define the incident velocity profile. The classical form of the semi-log velocity profile can be written as a function of height

(z) and given values for friction velocity (u_*), roughness height (Z_0), displacement height (d), and the von Karman constant (κ).

$$U(z) = \frac{u_*}{\kappa} \ln\left(\frac{z - d}{Z_0}\right) \quad (3)$$

If average building height of the domain is known, values for roughness height and displacement height can typically be acquired from existing literature on wind engineering, and the von Karman constant is generally set at a value of 0.4. The semi-logarithmic relationship is considered to be an acceptable model for velocity within the urban canopy and is frequently used in engineering solutions [26].

MODEL AND MESHING

Modelling a building of interest is one of the more straight-forward processes involved in a CFD simulation. Results from multiple studies investigating the effect of roof shape on airflow found that buildings with flat rooftops demonstrate the greatest energy harvesting potential for building mounted wind turbines [14,17,27]. The upstream edge of the roof is determined to have the most power potential and lowest turbulence intensity, although the final results should always be used to determine the optimal turbine location. Researchers also agree that the surrounding buildings have a significant impact on the available wind resources above a target rooftop, although the effects can be positive or negative depending on the specific case. When the target building is significantly taller than the surrounding buildings, the available energy from wind can nearly double [14]. Conversely, similar height buildings will see a reduction in wind power density. All buildings should be modelled at full size, as this is one of the core advantages of using a CFD approach. The shape of the roof edge also has a noticeable impact on simulation results [28]. Accurate modelling of the urban environment surrounding the turbine site is

essential for creating a realistic CFD simulation, otherwise significant errors may occur when attempting to obtain a complete wind behavior assessment [14]. As with any simulation, limitations on computing power must be considered when determining the level of detail for the model.

Meshing the building model and wind tunnel domain is another important step in the simulation setup. Generally, a finer mesh will result in higher quality results, so element size will always be a factor to consider. A proper mesh should be structured in an organized and uniform manner. Unstructured meshes consisting of pyramidal or tetrahedral elements tend to have issues with convergence [14]. Additional mesh refinement should be applied in specific areas of interest within the domain, such as the area above the rooftop, but not across the entire domain. The quality of a mesh may sometimes be limited by available computing resources. According to Toja-Silva, to verify the solution of a CFD study, the paper should at least include a convergence study of the mesh size and simulation results [14]. A more robust solution verification process involves the calculation of the Grid Convergence Index, but many published works do not go that far.

CHAPTER 3

INTRODUCTION TO OPENFOAM AND CFD SIMULATION

INTRODUCTION TO OPENFOAM

The open-source CFD software OpenFOAM was used to carry out the simulations. OpenFOAM simulations and associated parameters are defined by plain text files, which specify factors such as solver schemes, turbulence models, time step directories and controls, mesh and geometry files, bulk fluid properties, and more depending on the simulation being performed. Several solvers exist within the software that can be assigned by the user depending on the problem. Examples of some determining factors include the type of turbulence model needed, compressible or incompressible flow, considerations for heat transfer, steady-state versus transient cases, etc. Each case file begins with three primary folders;

- "systems" which contain text files for solver controls, schemes, meshing dictionaries, etc.
- "constant" which contains the geometry files and turbulence/transport properties
- "0" which represents the initial time step for the system and contains text files describing constant parameters, pressure and velocity, and others terms, depending on the solver.

OpenFOAM is a trusted software used for past and present academic research and commercial applications [14]. The fact that it is freely available and without licensing limitations is the reason that it was chosen for this study.

SIMULATION SETUP

The initial step in the setup process was to create a case file in OpenFOAM. The steady-state incompressible solver *simpleFoam* was used to carry out the simulations. The next step was to develop a 3D model of the high-rise building. An isolated building, modeled as a simple

rectangular prism, was created in the commercial CAD software Autodesk Inventor. The geometry was then exported as an STL file and placed in the *constant → trisurfaces* folder of the OpenFOAM case file. Gaussian second order upwind solvers were set by default in the *systems → fvSchemes* text file. The turbulence was set to realizeable k-epsilon model in the *constant → turbulence properties* text file. The domain setup for the wind tunnel was specified in the *system → blockMeshDict* text file. The block mesh defines the boundaries conditions for the simulation and constructs an initial mesh. An additional OpenFOAM meshing tool, *snappyHexMesh,* was used to generate detailed meshing on and around the building geometry and controls for the meshing tool can be found in the *system → snappyHexMeshDict* text file. Inlet velocity was specified in the *0 → U* text file. The simulation was set to run for 400 steps with a time-step of one second. Data was set to be recorded in intervals of 50 seconds. The simulations were carried out on two separate building orientations. One model was perpendicular to oncoming wind, and the other model was rotated 45 degrees. Simulation results were visualized and analyzed in the open-source software ParaView. Figure 2 displays wireframe images of the domain and buildings.

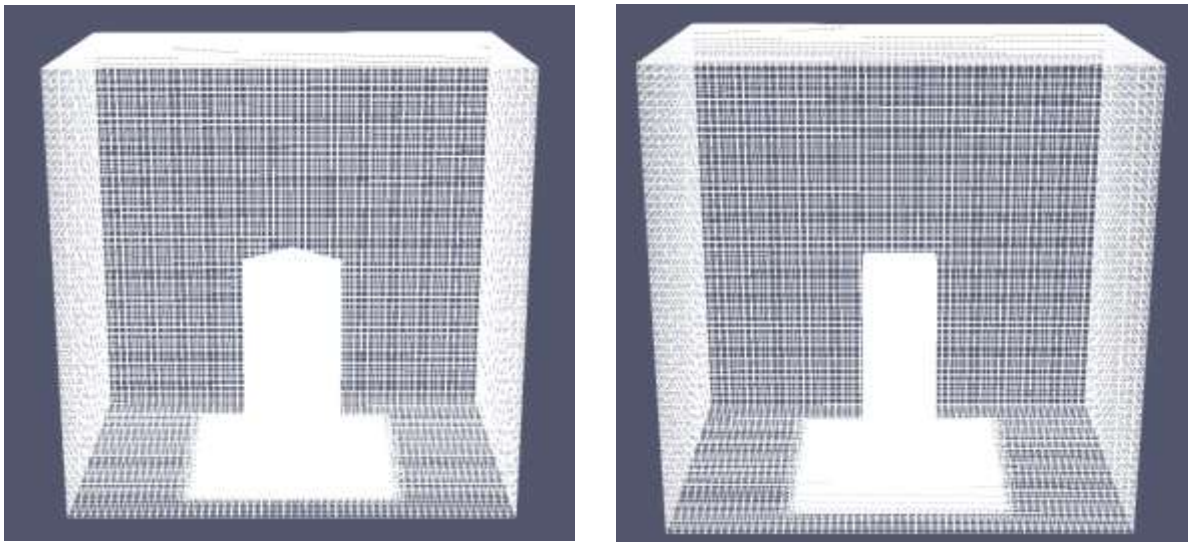

Figure 2: OpenFOAM Domain and Building Mesh

MESH ANALYSIS

To confirm that the results of the simulation are mesh independent, a mesh analysis was done using three different levels of mesh refinement. The coarse mesh had the least amount of refinement, containing only one refinement region and was approximately 5.6 million cells. The medium mesh had an inner level of increased refinement in the space around the building geometry and was approximately 7.2 million cells. Lastly, the fine mesh consisted of 8.6 million cells and had increased levels of refinement for both the inner and outer refinement regions. To test whether the results were mesh dependent, data for the target variable was recorded in the area of interest and compared across the different meshes. For this study, the wind velocity is the target variable, and the rooftop is the area of interest. The inlet velocity was set at 9 m/s (20 mph). Velocity was recorded along the upstream edge of the building (perpendicular to flow), and down the side edge of the building (parallel with flow) for each mesh level and compiled into a spreadsheet. A comparison of the recorded velocities is shown below in Figures 3 and 4.

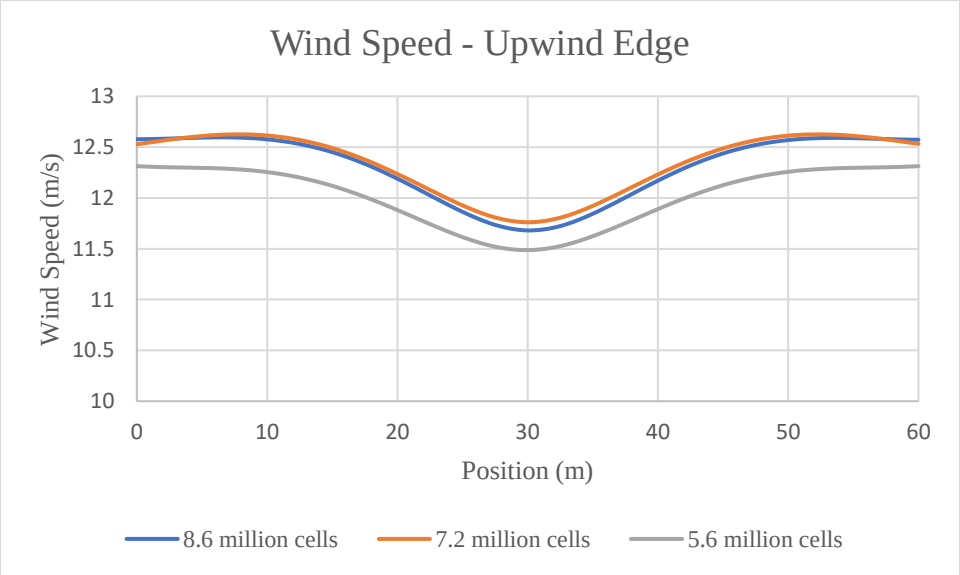

Figure 3: Mesh Comparison of Wind Speed Upwind Edge

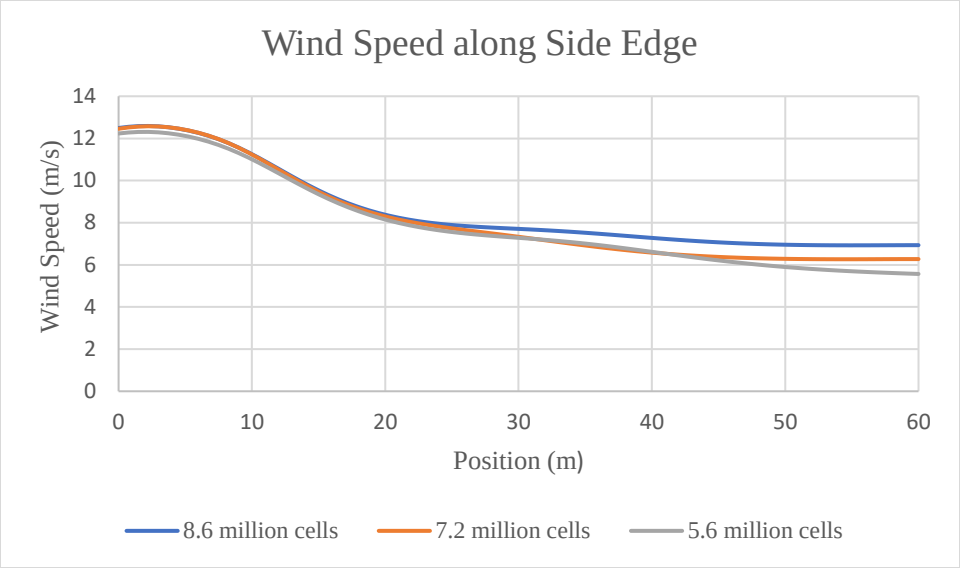

Figure 4: Mesh Comparison of Wind Speed Side Edge

The results show that the velocity along the upstream edge is nearly identical between the medium and fine meshes. There is a noticeable difference, although small, with the coarse mesh. For the side edge of the roof, the velocity recordings near the upstream corner and along the first half of the roof are negligibly different, however the velocities start to deviate along the downstream half of the rooftop. It is noteworthy that the velocity at the downstream edge increased as the mesh refinement was increased. For this study, only the upstream edge of the building will be analyzed for turbine performance. Results of the mesh analysis at three different refinement levels indicate that the medium mesh yields acceptable results and saves on computing time and power when compared to the finer mesh. Therefore, the medium mesh with 7.6 million cells was used to carry out the simulations. A cross-section of the mesh is shown below in Figure 5.

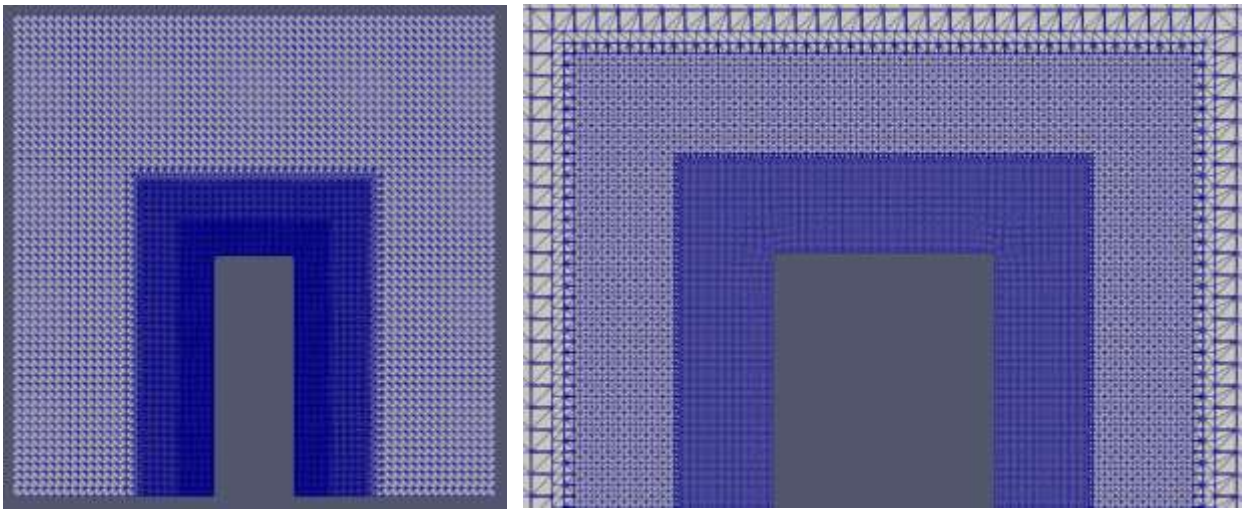

Figure 5: Final Mesh Cross Section View

RESULTS FOR ROOFTOP WIND SPEED

The goal in performing the CFD simulations was to develop a relationship between the incident wind speed and the wind speed above the rooftop at the turbine mounting location. To complete this, the inlet wind velocity was changed for each simulation and the rooftop speed along the upwind edge was recorded. The turbine manufacture specifies that the rotor of the turbine is 5 meters tall, and the mounting shaft for rooftops is 6 meters tall. This means that the center of the turbine rotor would sit 8.5 meters above the rooftop of a building that is 180 meters tall. A turbine installed on a rooftop would likely be a certain distance from the edge of the building to allow for maintenance access. A distance of 3 meters from the edge was determined to be a realistic amount of space. Therefore, data for velocity was recorded along the upstream edge of the building, offset 3 meters from the edge and 8.5 meters above the rooftop. The ranges for the incident wind speeds were chosen based on the range of operating wind speeds that are specified by the turbine manufacturer. The incident wind speed and the speed at the turbine location for both the perpendicular and 45 degree buildings are displayed in Table 1.

Table 1: Wind Speed Results of OpenFOAM Simulation

90° Building Incident Wind Speed (m/s)	Wind Speed at Turbine (m/s)	45° Building Incident Wind Speed (m/s)	Wind Speed at Turbine (m/s)
3.0	2.13	3.0	3.15
4.0	3.85	4.0	4.85
5.0	5.81	5.0	6.42
6.0	7.74	6.0	7.68
7.0	9.47	7.0	9.05
8.0	10.97	8.0	10.57
9.0	12.58	9.0	12.19
10.0	13.94	10.0	13.84
11.0	15.52	11.0	15.44
12.0	17.14	12.0	16.96
13.0	18.80	13.0	18.57
14.0	20.49	14.0	20.01
15.0	22.20	15.0	21.48

Using this data, a trendline was created between the two values using the incident wind speed as the independent variable and wind speed at the turbine as the dependent variable. Figures 6 and 7 contain a plot and trendline of the relationship for each building orientation.

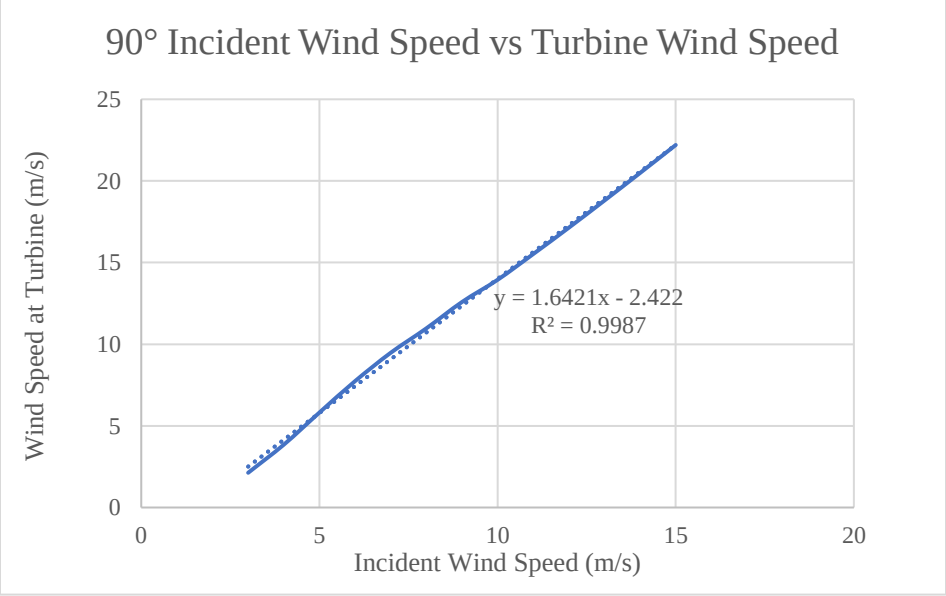

Figure 6: Incident vs Rooftop Wind Speed (90° Building)

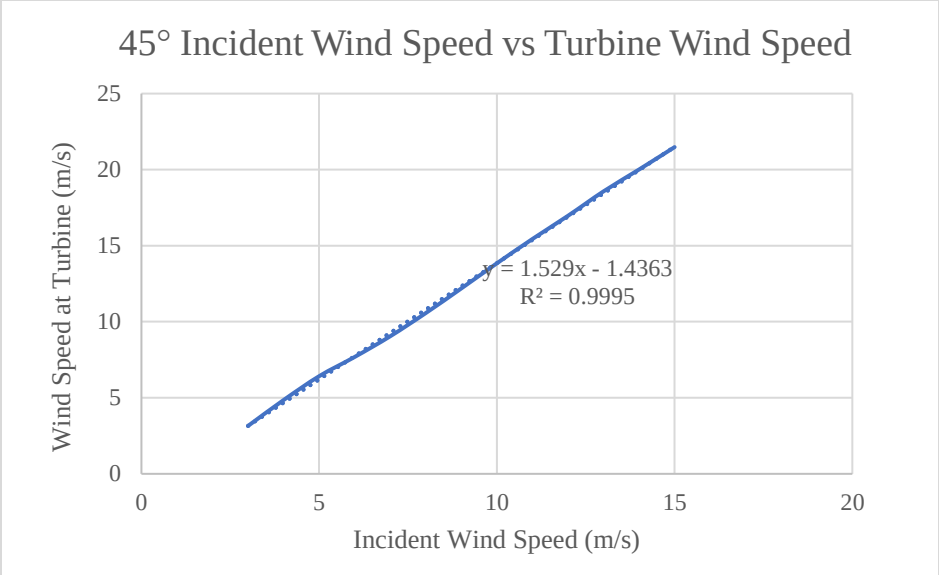

Figure 7: Incident vs Rooftop Wind Speed (45° Building)

The equations developed in Figures 6 and 7 will be used in conjunction with the reference wind data and the ABL velocity profile to determine the real wind speed at the turbine location. Both equations are provided below. The incident wind is at the height of the building, 180 m, and the elevation of the center of the turbine rotor is 188.5 meters. For wind perpendicular to the building, the velocity at turbine height is:

$$U_T = 1.6421 \times U(z_{180}) - 2.422 \quad (4)$$

And for wind 45 degrees to the building, the velocity at turbine height is:

$$U_T = 1.529 \times U(z_{180}) - 1.4363 \quad (5)$$

CHAPTER 4

VELOCITY PROFILE OF ATMOSPHERIC BOUNDARY LAYER

URBAN LAYOUT

The hypothetical turbine site for this study is a high rise building with a 1:1:3 ratio of 60-meter sides and 180 meters tall. The total domain is two city blocks by one and a half city blocks. The average city block is assumed to be 120 meters and a street width of 15 meters between blocks, for a total domain size of 270 meters by 202.5 meters. In order to create a more realistic urban landscape, varying dimensions were chosen for the surrounding buildings and some empty spaces were left in the domain to represent parking or other open areas commonly found in cities. All buildings besides the hypothetical turbine mounting site have ratios of either 1:1:1 or 1:1:2. A representation of the domain and buildings is shown below in Figure 8. The domain edge closest to the target building was assigned as the east edge and is adjacent to the body of water. The building dimensions and are given in Table 2.

Table 2: Building Dimensions of Urban Domain

Building No.	**Dimensions (m)**
1 (target)	60 x 60 x 180
2	40 x 40 x 80
3	60 x 60 x 60
4	50 x 50 x 100
5	30 x 30 x 60
6	40 x 40 x 40
7	45 x 45 x 90
8	35 x 35 x 70
9	50 x 50 x 50
10	40 x 40 x 40

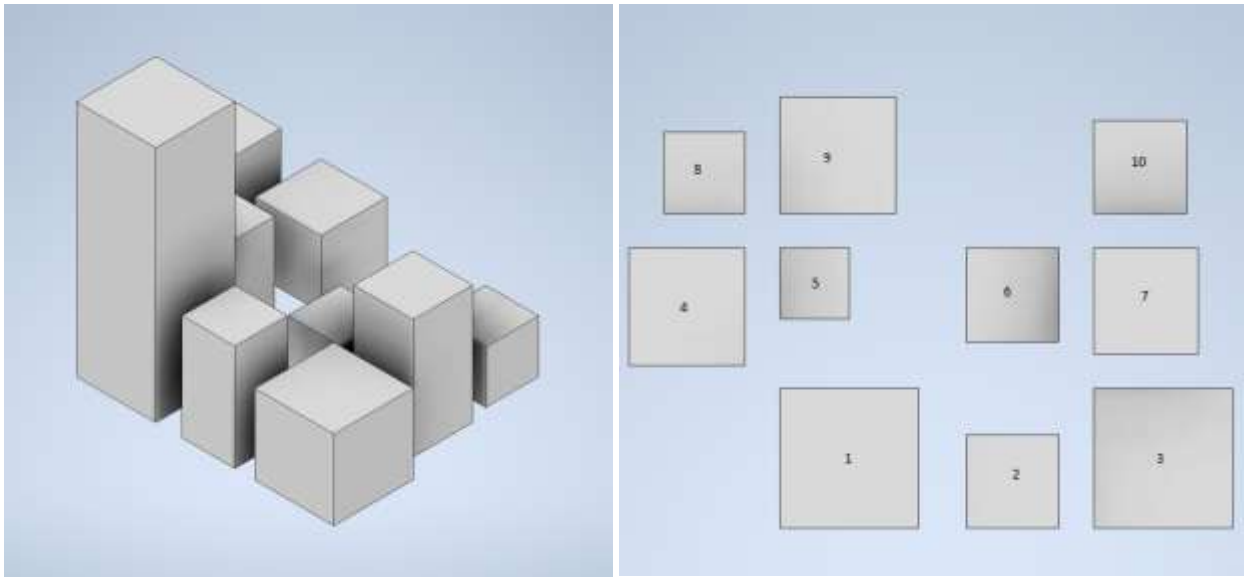

Figure 8: Representation of Urban Layout

The dimensions of the buildings and the domain were then used to calculate the front area density (λ_f), plane area density (λ_p), and the standard deviation of building height (σ_H). The front and plane area density values represent the ratio of building area to domain area. For plane area density, the rooftop areas are used, and for front area density the side face of each buildings is used. Calculated values for these parameters are provided in Table 3.

Table 3: Values for Urban Domain Parameters

Term	Value
λ_f	0.669
λ_p	0.387
σ_H	20.06

VELOCITY PROFILES

The amount of available wind energy is greatly affected by wind velocity, and as such the development of an accurate velocity profile is integral to performing an accurate analysis of turbine performance. ASHRAE has developed standards for wind within the atmospheric boundary layer, and these equations are generally accepted when it comes to engineering

practices. When the wind speed is known at a given height, then the velocity at any other height can be determined using the following equation provided by ASHRAE [29].

$$U = U_{ref}\left(\frac{\delta_{ref}}{Z_{ref}}\right)^{a_{ref}}\left(\frac{Z}{\delta}\right)^{a} \tag{6}$$

In this equation, U_{ref} represents the reference velocity at the given elevation Z_{ref}. The other two terms, δ and α represent the boundary layer thickness and an exponent determined by ASHRAE standards. Table 4 on the next page was taken from the ASHRAE SI Fundamentals Handbook [29].

Table 4: Atmospheric Boundary Layer Parameters

Terrain Category	**Description**	**Exponent α**	**Layer Thickness δ (m)**
1	Large city centers, in which at least 50% of buildings are higher than 25 m, over a distance of at least 0.8 km or 10 times the height of the structure upwind, whichever is greater.	0.33	460
2	Urban and suburban areas, wooded areas, or other terrain with numerous closely spaced obstructions having the size of single-family dwellings or larger, over a distance of at least 460 m or 10 times the height of the structure upwind, whichever is greater.	0.22	370
3	Open terrain with scattered obstructions having heights generally less than 9 m, including flat open country typical of meteorological station surroundings.	0.14	270
4	Flat, unobstructed areas exposed to wind flowing over water for at least 1.6 km, over a distance of 460 m or 10 times the height of the structure inland, whichever is greater.	0.10	210

As discussed previously, the exponential relationship for the boundary layer profile is not the most accurate solution for built environments with many tall structures. When analyzing the wind behavior around a building that is next to a large body of water, equation 6 will provide

adequate results for wind that is traveling from the water into the urban environment. However, when the wind is incident from the opposite direction, the wind speeds above the average building height will be underestimated by equation 6. Therefore, a modified semi-logarithmic profile, similar to equation 3, will be used for times when the incident wind is traveling from the city towards the water. The equations used in this study were modified by Heath et al. and are shown below, where the terms *d* and $Z_{0,ref}$ represent the displacement height and the surface roughness length of the reference location [30]. For this case, the reference location for wind incident from the city is assumed to be a suburban terrain with $Z_{0,ref}$ of 1.0 m.

$$U(z) = \frac{\ln\frac{(z-d)}{z_0}}{\ln\frac{(\delta-d)}{z_0}} \times \frac{\ln\frac{\delta}{z_{0,ref}}}{\ln\frac{z_{ref}}{z_{0,ref}}} \times U_{ref} \tag{7}$$

Additionally, δ can be calculated for the specific case using equation 8 below, where *x* represents the distance between the location of interest and the reference location. For this case *x* was approximated to be 2000 m. An approximation works well here, according to Heath et al. as *U* does not change significantly when *x* is greater than 1000 m.

$$\delta = 0.75 z_{0,ref} \left(\frac{x}{z_0}\right)^{0.8} \tag{8}$$

Before calculating velocity at the desired location and elevation, values must first be obtained for the displacement height *d* and the surface roughness length Z_0. The following equations developed by Macdonald et al. allow for the calculation of these parameters and are used in several studies [17, 26, 31].

$$\frac{d}{H_{ave}} = 1 + A^{\lambda_p}\left(\lambda_p - 1\right) \tag{9}$$

And

$$\frac{z_0}{H_{ave}} = \left(1 - \frac{d}{H_{ave}}\right) exp\left[-\left(0.5\beta \frac{C_D}{\kappa^2}\left(1 - \frac{d}{H_{ave}}\right)\lambda_f\right)^{-0.5}\right] \quad (10)$$

The coefficients *A*, β and C_D are equal to 4.43, 1.0, and 1.2 respectively. The term κ is the Von Karman constant and is equal to 0.4. Although widely used, the Macdonald equations were developed based on simple arrays of cubes rather than actual building arrangements. As a result, the solutions are not as accurate as they could be for a real setting. A study by Kanda et al led to the development of new parametric equations for *d* and Z_0 based on real urban settings. The researchers concluded that the new equations performed well for both realistic urban models and simplified models [32].

The equation for displacement height is

$$\frac{d}{H_{max}} = c_0 X^2 + \left(a_0 \lambda_p^{b_0} - c_0\right) \quad (11a)$$

Where X is given by

$$X = \frac{\sigma_H + H_{ave}}{H_{max}} \quad (11b)$$

And the relationship for surface roughness length is

$$\frac{z_0}{z_0(mac)} = b_1 Y^2 + c_1 Y + a_1 \quad (12a)$$

Where Y is given by

$$Y = \frac{\lambda_p \sigma_H}{H_{ave}} \quad (12b)$$

The coefficients a_0, b_0 and c_0 are constant parameters with values of 1.29, -0.17, and 0.36 and a_1, b_1 and c_1 are constant parameters with values of 0.71, 20.21 and -0.77, respectively. H_{ave} and H_{max} are the average and maximum building heights, σ_H is the standard deviation in building height, and λ_p is the plane area density of the building arrangement. $Z_{0(mac)}$ is the roughness length calculated using the Macdonald equations. Table 5 contains the calculated values for *X, Y, d,* $Z_{0(mac)}$, Z_0 and δ.

Table 5: Values of Velocity Profile Parameters

Term	Value
X	0.48
Y	0.118
d	114.8 (m)
$Z_{0(mac)}$	7.71 (m)
Z_0	6.94 (m)
δ	483 (m)

CHAPTER 5

ENERGY PRODUCTION OF TURBINE

REFERENCE WIND DATA

The concept for the building was based on a location along Lake Michigan in Chicago, IL. The location was chosen because of the detailed wind data over Lake Michigan, provided by the NOAA Great Lakes Environmental Research Laboratory, that is publicly available online, and the layout of downtown Chicago fits the image of a classical city environment with many tall buildings. The wind data produced by the NOAA is recorded every two minutes and includes several characteristics of the flow, including the wind speed and direction. The data from the calendar year 2020 was chosen for this study. To simplify the calculations, the data was organized in Microsoft Excel to provide hourly averages of wind speed and direction. A sample of the hourly averaged data for one day is shown below in Table 6. The anemometer used to record the data is 2.75 miles from the Chicago shoreline at an elevation of 25.9 meters (Z_{ref}).

Table 6: Sample of Reference Wind Data

Hour	**Avg Direction (deg)**	**Avg Speed (m/s)**	**Hour**	**Avg Direction (deg)**	**Avg Speed (m/s)**
1	264.23	11.00	13	250.67	7.51
2	272.53	10.42	14	239.73	7.35
3	270.33	9.91	15	214.20	9.56
4	264.20	9.05	16	206.47	8.95
5	268.97	8.86	17	197.67	8.87
6	272.30	8.06	18	195.47	9.01
7	271.87	8.18	19	199.13	8.92
8	266.27	8.36	20	197.67	9.76
9	261.93	7.65	21	194.60	10.78
10	253.20	6.91	22	194.97	12.79
11	248.47	6.51	23	190.60	12.85
12	249.53	7.15	24	193.47	12.46

TURBINE SPECIFICATIONS

The commercial VAWT chosen for this study is the QuietRevolution QR6 wind turbine. The QR6 is a helical Darrieus wind turbine with three blades. The design of the turbine is intended to minimize noise and vibrations from device and achieve a lower the start-up wind speed. The QR6 is rated for 7 kilowatts and a cut in speed of approximately 2 m/s (4.5 mph) and a safety cut-out of approximately 20 m/s (45 mph). A power curve for the turbine provided by the manufacturer is shown below in Figure 9. Using the curve from the manufacturer, an equation was produced in excel for use in the power calculations. The recreated curve and equation is shown in Figure 10.

Figure 9: QR6 Power Curve (Manufacturer)

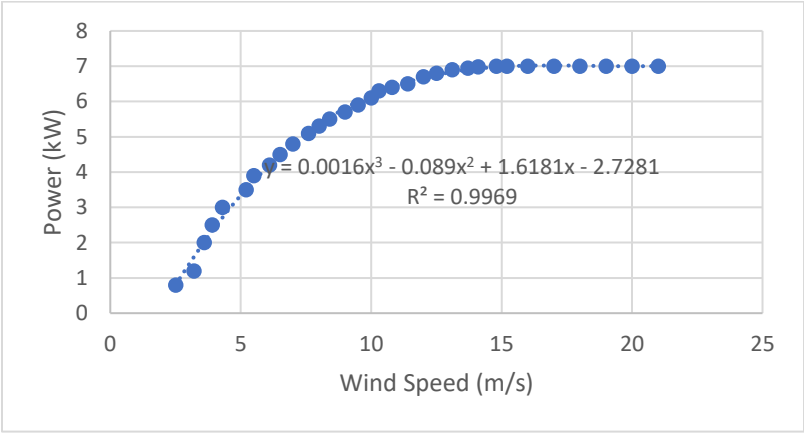

Figure 10: Recreated QR6 Power Curve

The power produced by the turbine, as a function of wind speed, is given by the equation

$$P_{kW} = 0.0016U_T^3 - 0.089U_T^3 + 1.6181U_T - 2.7281 \quad (13)$$

The direction of the wind for each hour was used to assign that hour to one of 10 regions: east, north-east, north (lake), north (city), north-west, west, south-west, south (city), south (lake) and south-east. The body of water is east of the building, and the city is west of the building. The shoreline is considered to be a north-south line. A breakdown of each direction and the assumptions made for determining which equations to use are provided in Table 7. Both the north and south directions were divided into two regions to define wind incident from the city or the water.

Table 7: Summary of Characteristics for Reference Wind Data

Direction	Degree Range	City/Lake Wind	Simulated Building
N (lake)	0° - 22.49°	Lake	90°
NE	22.5° - 67.49°	Lake	45°
E	67.5° - 112.49°	Lake	90°
SE	112.5° - 157.49°	Lake	45°
S (lake)	157.5° - 179.99°	Lake	90°
S (city)	180° - 202.49°	City	90°
SW	202.5° - 247.49°	City	45°
W	247.5° - 292.49°	City	90°
NW	292.5° - 337.49°	City	45°
N (city)	337.5° - 359.99°	City	90°

ENERGY YIELD

To calculate the energy production of the turbine, the averaged hourly wind speeds from the NOAA data were entered into the appropriate velocity profile equation (Equation 6 or Equation 7 depending on the wind direction) to determine the incident wind speed at the rooftop height of 180 meters (U_{180}). The incident wind speed is then used in Equation 4 or Equation 5 (again depending on wind direction) to determine the wind speed at the turbine location, U_T.

Finally, U_T is plugged into Equation 13 to determine the average rate of power production for that hour. Table 8 contains the results of the power production calculations, including the hours during the year where the average wind speed at the turbine location was either below the cut-in speed or above the safety cut-off speed specified by the turbine manufacturer.

Table 8: Summary of Power Calculations

Direction	**# of hours**	**Power Produced (kWh)**
N (lake)	323	2,168
NE	757	4,032
E	686	3,403
SE	780	3,936
S (lake)	584	3,199
S (city)	740	4,493
SW	1,042	6,208
W	1,301	7,462
NW	1,066	6,031
N (city)	271	1,625
Null Hours	1,234	0
Total	**8,784**	**42,557**

CHAPTER 6

TURBINE SPACING

SIMULATION OF ROTATING TURBINE

To ensure that a turbine is operating as efficiently as possible, it is important to consider the interference in air flow caused by neighboring turbines. For this study, the downstream behavior of air flow was analyzed using OpenFOAM. The first step in creating the CFD model was to create a solid model of the QR6 blades. The specifications for the blades were taken from an existing study and can be found in Table 9 [33]. The airfoil profile used was the NACA 0018. Values representing the airfoil shape were imported into Inventor and extruded helically to create the blades. Once the blades were modeled and exported, the geometry file was placed in the *trisurface* folder for the CFD simulation. In addition to importing the blades, a rotating mesh needed to be developed to simulate a turbine in operation. In order to accomplish this, a solid cylinder was modeled in Inventor and exported for use in the *trisurface* folder, similar to the turbine blades. The cylinder was then used to define an Arbitrary Mesh Interface, or AMI, which represent the rotating cells in the final mesh. The domain for the simulation was created using the *-blockMesh* command and the blade and AMI geometry were created using the *-snappyHexMesh* command. Further levels of refinement were added to the blades and the AMI to make the simulation more accurate. Images of the turbine blades and the final mesh are shown in Figure 11.

Table 9: Rotor Parameters [33]

Height	5.5 m
Diameter	3.1 m
Swept area	16 m^2
Chord length	0.195 m
Airfoil	NACA 0018
Helical angle	120°

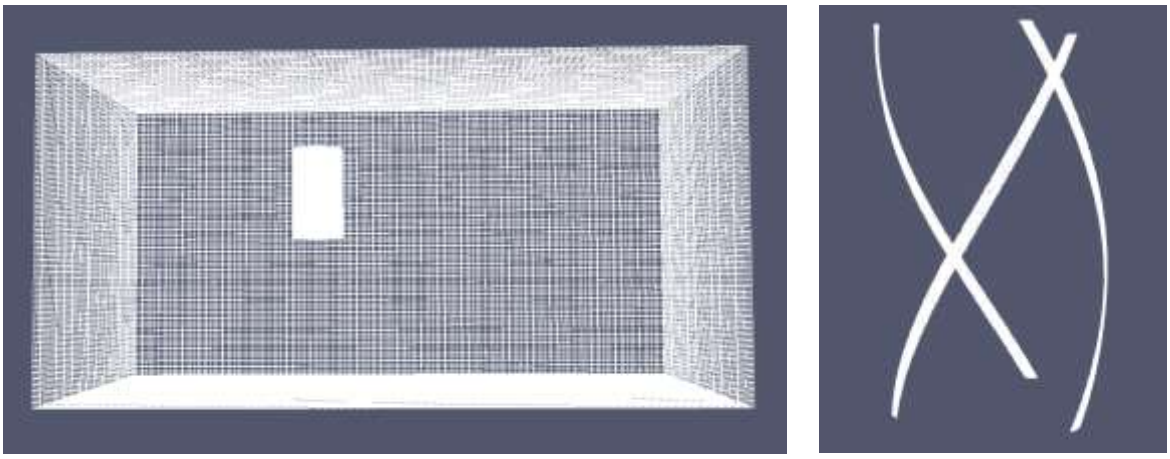

Figure 11: Final Mesh and Rotor Blades

Once the geometry and mesh were developed, the parameters of the simulation were defined. According to the manufacturer, the QR6 is designed to perform in winds up to 20 m/s (45 mph) and a maximum rotations per minute of 260. Therefore, the rotating zone of the mesh was set at the maximum RPM and the inlet wind velocity for the domain was set to the maximum operating speed. The transient OpenFOAM solver *pimpleFoam* was used for this simulation. The solver schemes used Gaussian second order upwind equations and the solver time step was set as 0.0005 seconds. An image of the completed simulation is shown in Figure 12.

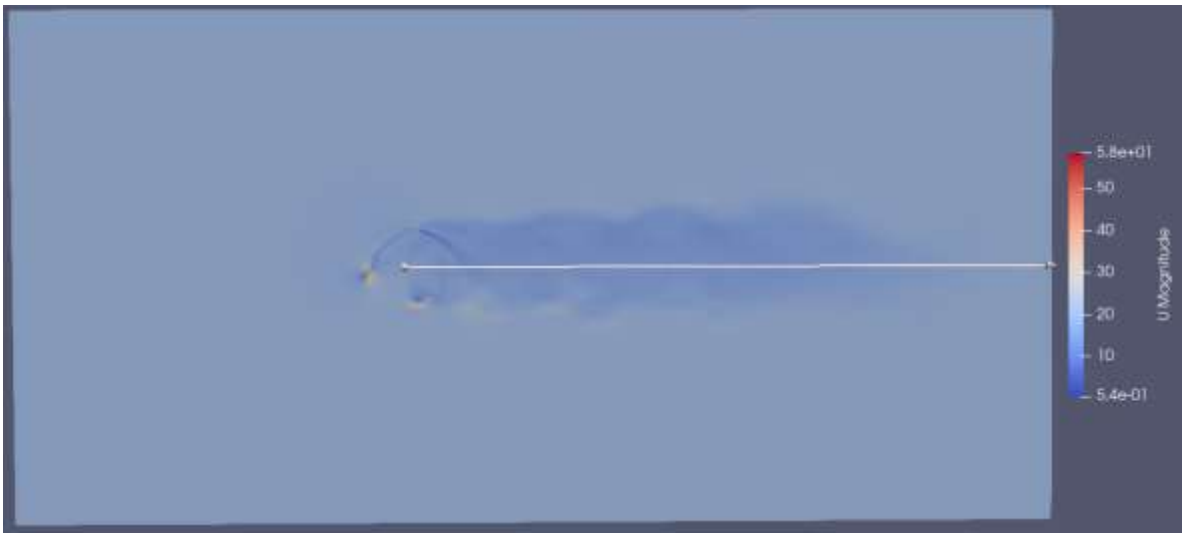

Figure 12: OpenFOAM Simulation of Rotating Turbine

SIMULATION RESULTS

Figure 13 displays the change in velocity along the center line using data recorded from the OpenFOAM simulation. A significant drop in velocity occurs until approximately 15 meters from the turbine center, at which point the velocity begins to increase towards the free stream value. Table 10 compares values between actual velocity and free stream velocity from 15 to 24 m downstream from the turbine center. The velocity is mostly steady 10 to 15 m downstream, at about 80 percent of the maximum. Velocity oscillates unsteadily from 0 to 9 m downstream.

Table 10: Velocity Results Downstream of Turbine

Distance (m)	**U (m/s)**	**U/U∞**
15	16.115	0.806
16	16.608	0.830
17	17.043	0.852
18	17.469	0.873
19	17.867	0.893
20	18.420	0.921
21	19.057	0.953
22	19.570	0.978
23	19.866	0.993
24	19.950	0.997

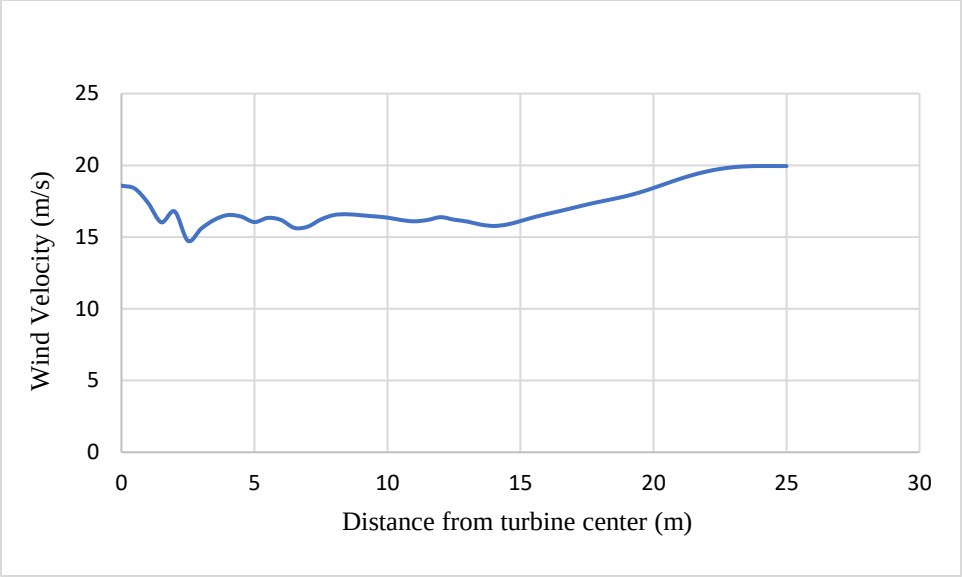

Figure 13: Downstream Velocity vs Distance from Turbine

CHAPTER 7

BUILDING VIBRATIONS

MODAL ANALYSIS OF STEEL FRAME

The impact of turbine vibration on the structure must be considered for a rooftop installation. For this study, a simple modal analysis of the beam structure of the building is performed and compared with an existing modal analysis of a vertical axis turbine rotor . The beam model and frame analysis were created using the commercial CAD software Autodesk Inventor. For simplicity, a uniform beam size was chosen to create the model, based on the dimensions of the building. The beam size used is ANSI W – 18x71 steel beams, and the model consists of 5404 beam elements. The specifications for beam size were chosen based on recommendation from an architect. Images of the beam model are shown below in Figure 14.

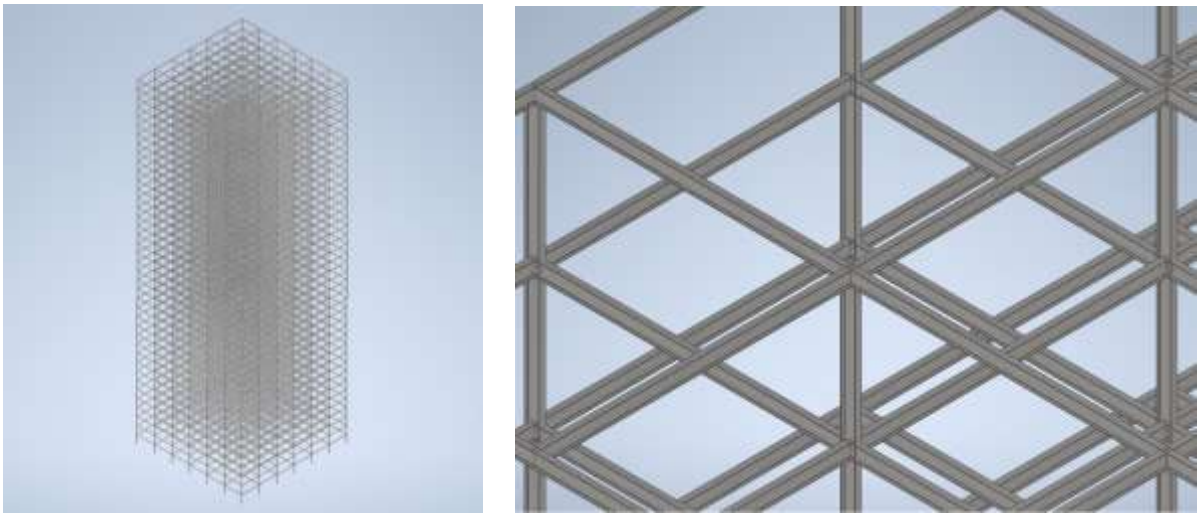

Figure 14: Beam Model of Isolated Building

To perform the modal analysis, the frame analyzing tool was used in Inventor. Each of the 49 vertical columns were set as fixed supports at the base of the building. The simulation was performed over eight iterations at a tolerance of 0.001 and the number of modes calculated

was eight. Table 11 displays the numerical results of the simulation, and the visual result of an example mode is shown in Figure 15.

Table 11: Results of Building Modal Analysis

Mode Number	Frequency (Hz)	Maximum Displacement (in.)
1	0.08	0.0261
2	0.15	0.0435
3	0.22	0.0309
4	0.25	0.0274
5	0.36	0.0397
6	0.38	0.0377
7	0.44	0.0299
8	0.52	0.0367

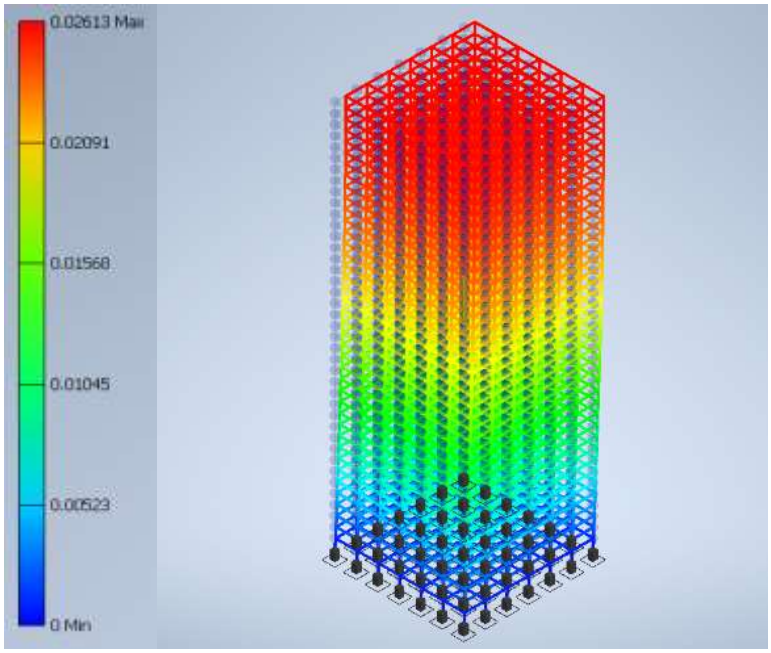

Figure 15: Example of Modal Analysis (Mode 1, 0.08 Hz)

CHAPTER 8

DISCUSSION OF RESULTS

DISCUSSION OF ENERGY YIELD

Regarding the power production of the turbine, the results of the calculations indicate that rooftop mounted VAWTs could be a promising source of on-site renewable energy generation. The accelerated flow over the top of the building is confirmed by the velocity results of the CFD simulations, and faster wind leads to more power from the turbine. For this study, there was only one turbine in the model, and the power output was calculated at 4 different corners of the building. Clearly this is not a realistic scenario, but it still provides useful insight into the potential performance that one could expect with a rooftop turbine installed. For a more realistic setup, data should be collected along all edges of the building for each velocity and building orientation. Turbines could then be stationed along the perimeter of the roof and a total energy yield of the array could be calculated. Although the wind speed on the downstream edge of the building will be slower than the upstream edge, power would still be generated at a lesser rate. For example, Figure 4 from the mesh analysis shows that the wind velocity on the downstream corner of the building is approximately 7 m/s (15.5 mph), which translates to a rate of 4 – 5 kilowatts of power produced, according to the manufacturer power curve. The mesh analysis was performed with an incident velocity of 9 m/s (20 mph), which is in the middle of the operating range of the turbine.

The cost of electricity in Chicago for May 2020 was $0.15/kWh. The calculations performed in this study assume that the turbine is always on the upstream edge of the building, which is not a realistic case. Although the mesh convergence was not performed for the downstream edge, Figure 4 still provides an estimate of the decrease in wind speed that will

occur as wind travels across the rooftop. Using this downstream wind speed (approximately 7 m/s or 15.5 mph) and the power curve provided by the manufacturer, it can be roughly estimated that a downstream turbine will produce 30 to 40 percent less power than a turbine on the leading edge. Therefore, a real roof mounted QR6 turbine would still produce roughly 30,000 kWh annually, which is a monetary value of $4,500 in electricity. The QR6 is an expensive wind turbine at around $55,000 according to listings found online. The electricity produced would pay for the purchase price of the turbine in 12 to 13 years if prices remained steady. However, continued research and interest in VAWTs will hopefully lead to reduced turbine prices in the future. It should be noted that the price of electricity can vary greatly between locations, and from year to year, so any real cost analysis should be performed on a case-by-case basis.

DISCUSSION OF TURBINE SPACING

The results from the turbine spacing simulation indicate that approximately 22 meters from the turbine center, the downstream velocity reaches roughly 98% of the free stream velocity. A downwind turbine placed closer than this distance would still produce power, although at a reduced rate. To maximize the power generated by an array of turbines within a defined space (rooftop), further analysis would need to be performed to optimize the combination of turbine spacing and power production per turbine. For the QR6 turbine, the manufacturer recommends a spacing of three turbine diameters, which is about 9 meters. This is well below the distances found in the simulation, although the manufacture does not say that zero interference will occur at the suggested spacing, only minimize the impact each turbine has on neighboring turbines. It can be seen from the simulation results that the wind speed oscillates until around 9 meters from the turbine, so it is possible that the manufacturer chose that distance as the location where wind speed becomes steadier. A turbine would still produce useful power

at the reduced wind speeds. It is also worth mentioning that researchers have published works suggesting that using synergized clusters of turbines with closer spacing and opposite directions of rotation can increase performance and overall yield [34].

DISCUSSION OF MODAL ANALYSIS

The only real conclusions that can be drawn from the modal analysis are that the turbine should have no impact on the structural integrity of the building frame. Relevant literature indicates that VAWTs have a natural frequency range that is much higher than those observed for the building frame [33]. If there were to be any effects of vibration between the turbine and building, they would be localized to the turbine location. The turbine frequency range may cause vibrations to the structure that could be perceptible by humans [35]. A more detailed analysis would need to be performed on individual floors of the building, using a more realistic model of the building including all construction materials. This would likely require assistance from structural engineers and/or architects with deeper knowledge of building construction.

Knowing the natural frequencies of the structure can aid the engineer or designer in selection and installation of a turbine. If the rotating turbine resonates with the natural frequency of the building structure, and the amplitude is great enough, it may cause occupant discomfort or even structural damage to the building. In an ideal scenario, the best method for analyzing these effects would involve field tests. Multiple accelerometers should be placed at points of interest on the structure, from which data could be collected to determine the amplitude of any resonance occurring between structure and turbine. If the vibration data for a chosen turbine is known, a more detailed simulation may be performed by adding external loads to the beam model analysis. Additionally, controlled damping may be implemented to a turbine in the form of a decoupler, which can reduce the impact of vibration on the structure [36].

CHAPTER 9

SUMMARY AND CONCLUSIONS

The objective of this study was to use computational fluid dynamics simulations to evaluate the performance of a vertical axis wind turbine on the rooftop of a building set in a dense urban environment. The city environment was also near a large body of water. Background research was done on the history of wind turbines, the various types of turbine designs, and the practice of using computational fluid dynamics for wind engineering. Real wind data recorded over Lake Michigan by the NOAA Great Lakes Environmental Research Laboratory was used as the reference data for performing the evaluation. Once the site and reference data were determined, a model was developed using a combination of the commercial CAD software Autodesk Inventor and the open-source CFD software OpenFOAM. Data from the CFD simulations was then analyzed and recorded using the multi-platform software ParaView. Next, velocity profiles for the atmospheric boundary layer were developed. Two profiles were created – one for wind traveling over water, and another for wind traveling over the urban canopy. The velocity profiles were used to determine the incident wind speed at building height, based on the reference wind conditions from the NOAA dataset. The wind speed at building height was then used to calculate the rooftop velocity, according to results from the CFD simulations. This velocity was then inserted into the power equation for the specified wind turbine and energy production was calculated. Calculations were done using hourly averages of wind data from the year 2020, which consisted of 8,784 hours. A total annual energy output was determined and analyzed against the cost of electricity and the price of the turbine.

In addition to the calculation of energy yield, two brief analyses were performed on the vibrations of the building structure and on the spacing of turbines for optimal use. The vibration

analysis was done using Autodesk Inventor. A basic steel frame of the target building was developed, and a modal analysis performed using the frame analysis tool. For the turbine spacing simulation, a simple model of the helical turbine was created in Inventor and inserted into the CFD case files in OpenFOAM. A cyclic AMI was defined within the case file to create a rotating mesh consisting of the rotor cylinder and blades. The downstream velocity was recorded and turbine spacing was discussed based on these results, as well as the recommendations of the turbine manufacturer.

The calculated energy yield, although not entirely realistic, confirms the feasibility of a commercial VAWT installed on an urban rooftop as a renewable energy source. The methodology used in this study could be applied to specific sites and offers a quicker and more cost-effective way to research potential turbine locations. Future work should include a more realistic calculation of the turbine performance, including an array of turbines at fixed locations, rather than assuming each case to be at the upwind edge of the building. Additionally, synergistic turbine clustering is an interesting concept to increase performance and could easily be applied on a large rooftop. If research on wind devices continues and associated costs are reduced, the installation of rooftop VAWTs should be considered as a green energy solution for urban environments.

REFERENCES

[1] Aznar, A., Day, M., Doris, E., Donohoo-vallett, P., Aznar, A., Day, M., Doris, E., and Donohoo-vallett, P., 2015, "City-Level Energy Decision Making: Data Use in Energy Planning, Implementation, and Evaluation in U.S. Cities - 64128.Pdf," (July).

[2] Kaldellis, J. K., and Zafirakis, D., 2011, "The Wind Energy (r)Evolution: A Short Review of a Long History," Renew. Energy.

[3] IRENA, 2019, *Renewable Energy Statistics 2019*.

[4] Ahmed, N. A., and Cameron, M., 2014, "The Challenges and Possible Solutions of Horizontal Axis Wind Turbines as a Clean Energy Solution for the Future," Renew. Sustain. Energy Rev.

[5] Kumar, R., Raahemifar, K., and Fung, A. S., 2018, "A Critical Review of Vertical Axis Wind Turbines for Urban Applications," Renew. Sustain. Energy Rev., **89**(March), pp. 281–291.

[6] Toja-Silva, F., Colmenar-Santos, A., and Castro-Gil, M., 2013, "Urban Wind Energy Exploitation Systems: Behaviour under Multidirectional Flow Conditions - Opportunities and Challenges," Renew. Sustain. Energy Rev., **24**, pp. 364–378.

[7] Grogg, K., 2005, "Harvesting the Wind : The Physics of Wind Turbines Harvesting the Wind : The Physics of Wind Turbines," Wind Energy, pp. 1–44.

[8] Ragheb, M., and M., A., 2011, "Wind Turbines Theory - The Betz Equation and Optimal Rotor Tip Speed Ratio," *Fundamental and Advanced Topics in Wind Power*.

[9] Tummala, A., Velamati, R. K., Sinha, D. K., Indraja, V., and Krishna, V. H., 2016, "A Review on Small Scale Wind Turbines," Renew. Sustain. Energy Rev., **56**, pp. 1351–1371.

[10] Aslam Bhutta, M. M., Hayat, N., Farooq, A. U., Ali, Z., Jamil, S. R., and Hussain, Z., 2012, "Vertical Axis Wind Turbine - A Review of Various Configurations and Design Techniques," Renew. Sustain. Energy Rev., **16**(4), pp. 1926–1939.

[11] Zemamou, M., Aggour, M., and Toumi, A., 2017, "Review of Savonius Wind Turbine Design and Performance," Energy Procedia, **141**, pp. 383–388.

[12] Kumar, P. M., Sivalingam, K., Narasimalu, S., Lim, T.-C., Ramakrishna, S., and Wei, H., 2019, "A Review on the Evolution of Darrieus Vertical Axis Wind Turbine: Small Wind Turbines," J. Power Energy Eng., **07**(04), pp. 27–44.

[13] Casini, M., 2015, "Small Vertical Axis Wind Turbines for Energy Efficiency of Buildings," J. Clean Energy Technol., **4**(1), pp. 56–65.

[14] Toja-Silva, F., Kono, T., Peralta, C., Lopez-Garcia, O., and Chen, J., 2018, "A Review of Computational Fluid Dynamics (CFD) Simulations of the Wind Flow around Buildings for Urban Wind Energy Exploitation," J. Wind Eng. Ind. Aerodyn., **180**, pp. 66–87.

[15] Emejeamara, F. C., Tomlin, A. S., and Millward-Hopkins, J., 2015, "Urban Wind: Characterization of Useful Gust and Energy Capture," Renew. Energy, **81**, pp. 162–172.

[16] McIntosh, S. C., Babinsky, H., and Bertényi, T., 2007, "Optimizing the Energy Output of Vertical Axis Wind Turbines for Fluctuating Wind Conditions," Collect. Tech. Pap. - 45th AIAA Aerosp. Sci. Meet., **23**(January), pp. 16202–16214.

[17] Ledo, L., Kosasih, P. B., and Cooper, P., 2011, "Roof Mounting Site Analysis for Micro-Wind Turbines," Renew. Energy, **36**(5), pp. 1379–1391.

[18] Balduzzi, F., Bianchini, A., Carnevale, E. A., Ferrari, L., and Magnani, S., 2012, "Feasibility Analysis of a Darrieus Vertical-Axis Wind Turbine Installation in the Rooftop of a Building," Appl. Energy, **97**, pp. 921–929.

[19] Rezaeiha, A., Montazeri, H., and Blocken, B., 2020, "A Framework for Preliminary Large-Scale Urban Wind Energy Potential Assessment: Roof-Mounted Wind Turbines," Energy Convers. Manag., **214**(October 2019), p. 112770.

[20] REN21 community, 2019, *Renewables 2019 Global Status Report*.

[21] Dominy, R. G., Lunt, P., Bickerdyke, A., and Dominy, J., 2007, "Self-Starting Capability of a Darrieus Turbine," Proc. Inst. Mech. Eng. Part A J. Power Energy.

[22] Stathopoulos, T., Alrawashdeh, H., Al-Quraan, A., Blocken, B., Dilimulati, A., Paraschivoiu, M., and Pilay, P., 2018, "Urban Wind Energy: Some Views on Potential and Challenges," J. Wind Eng. Ind. Aerodyn.

[23] Blocken, B., 2014, "50 Years of Computational Wind Engineering: Past, Present and Future," J. Wind Eng. Ind. Aerodyn.

[24] Toja-Silva, F., Peralta, C., Lopez-Garcia, O., Navarro, J., and Cruz, I., 2015, "Roof Region Dependent Wind Potential Assessment with Different RANS Turbulence Models," J. Wind Eng. Ind. Aerodyn., **142**, pp. 258–271.

[25] Romanić, D., Rasouli, A., and Hangan, H., 2015, "Wind Resource Assessment in Complex Urban Environment," Wind Eng., **39**(2), pp. 193–212.

[26] Macdonald, R. W., 2000, "Modelling the Mean Velocity Profile in the Urban Canopy Layer," Boundary-Layer Meteorol., **97**(1), pp. 25–45.

[27] Tabrizi, A. B., Whale, J., Lyons, T., and Urmee, T., 2014, "Performance and Safety of Rooftop Wind Turbines: Use of CFD to Gain Insight into Inflow Conditions," Renew. Energy.

[28] Toja-Silva, F., Peralta, C., Lopez-Garcia, O., Navarro, J., and Cruz, I., 2015, "On Roof Geometry for Urban Wind Energy Exploitation in High-Rise Buildings," Computation.

[29] Ashrae, 2009, *ASHRAE Handbook - Fundamentals (SI Edition)*.

[30] Heath, M. A., Walshe, J. D., and Watson, S. J., 2007, "Estimating the Potential Yield of Small Building-Mounted Wind Turbines," Wind Energy, **10**(3), pp. 271–287.

[31] Drew, D. R., Barlow, J. F., and Cockerill, T. T., 2013, “Estimating the Potential Yield of Small Wind Turbines in Urban Areas: A Case Study for Greater London, UK,” J. Wind Eng. Ind. Aerodyn.

[32] Kanda, M., Inagaki, A., Miyamoto, T., Gryschka, M., and Raasch, S., 2013, “A New Aerodynamic Parametrization for Real Urban Surfaces,” Boundary-Layer Meteorol., **148**(2), pp. 357–377.

[33] Bostan, V., Guţu, M., and Rabei, I., 2018, “Development and Validation of a CFD Model Used for Vertical Axis Wind Turbines Simulations,” IOP Conf. Ser. Mater. Sci. Eng., **444**(2).

[34] Hezaveh, S. H., Bou-Zeid, E., Dabiri, J., Kinzel, M., Cortina, G., and Martinelli, L., 2018, “Increasing the Power Production of Vertical-Axis Wind-Turbine Farms Using Synergistic Clustering,” Boundary-Layer Meteorol., **169**(2), pp. 275–296.

[35] Sampaio, R. A., and De Souza, R. M., 2015, “Vibration Analysis of a Residential Building,” MATEC Web Conf., **24**(January).

[36] Castellani, F., Astolfi, D., Peppoloni, M., Natili, F., Buttà, D., and Hirschl, A., 2019, “Experimental Vibration Analysis of a Small Scale Vertical Wind Energy System for Residential Use,” Machines, **7**(2), pp. 1–19.

APPENDIX A

NACA0018 AIRFOIL PROFILE COORDINATES

NACA 0018	
1	0.00189
0.95	0.0121
0.9	0.02172
0.8	0.03935
0.7	0.05496
0.6	0.06845
0.5	0.07941
0.4	0.08705
0.3	0.09003
0.25	0.08912
0.2	0.08606
0.15	0.08018
0.1	0.07024
0.075	0.063
0.05	0.05332
0.025	0.03922
0.0125	0.02841
0	0
0.0125	-0.02841
0.025	-0.03922
0.05	-0.05332
0.075	-0.063
0.1	-0.07024
0.15	-0.08018
0.2	-0.08606
0.25	-0.08912
0.3	-0.09003
0.4	-0.08705
0.5	-0.07941
0.6	-0.06845
0.7	-0.05496
0.8	-0.03935
0.9	-0.02172
0.95	-0.0121
1	-0.00189

APPENDIX B

LOCATION OF ANEMOMETER FOR WIND DATA

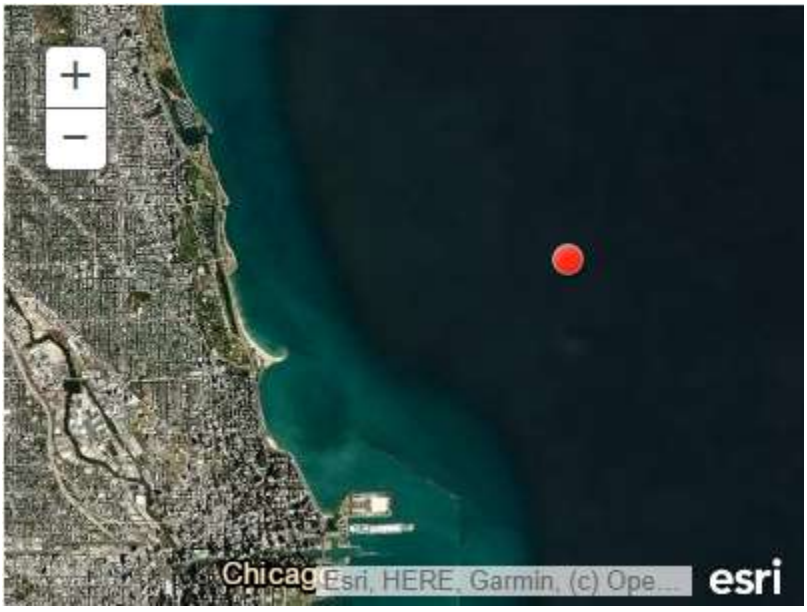

VITA

Graduate School

Southern Illinois University

Kyle R. Ozier

kozier94@outlook.com

Southern Illinois University Carbondale

Bachelor of Science, Mechanical Engineering, May 2017

Thesis Title: ESTIMATING THE POWER PRODUCED BY A ROOF MOUNTED WIND TURBINE IN AN URBAN SETTING

Major Professor: Dr. James Mathias